Structural Engineering and Mechanics, *Vol. 62, No. 3 (2017) 311-324*
DOI: https://doi.org/10.12989/sem.2017.62.3.311

Bending analysis of functionally graded plates using new eight-unknown higher order shear deformation theory

Tran Minh Tu*[1], Tran Huu Quoc[1a] and Nguyen Van Long[2b]

[1]*National University of Civil Engineering, 55 Giai Phong Road, Hanoi, Vietnam*
[2]*Construction Technical College No.1, Trung Van, Tu Liem, Hanoi, Vietnam*

(Received February 20, 2016, Revised January 9, 2017, Accepted January 13, 2017)

Abstract. In this paper a new eight-unknown higher order shear deformation theory is proposed for functionally graded (FG) material plates. The theory based on full twelve-unknown higher order shear deformation theory, simultaneously satisfy zeros transverse stresses at top and bottom surface of FG plates. Equations of motion are derived from principle of virtual displacement. Exact closed-form solutions are obtained for simply supported rectangular FG plates under uniform loading. The accuracy of present numerical results has been verified by comparing it with generalized shear deformation theory. The effect of power law index of functionally graded material, side-to-thickness ratio, and aspect ratio on static behavior of FG plates is investigated.

Keywords: bending analysis; functionally graded materials; higher order shear deformation theory; closed-form solution

1. Introduction

Functionally graded materials (FGMs) are new types of composite materials whose mechanical properties vary continuously through a certain direction; and thus avoid the delamination in the laminated composite materials. Typical FGMs are made from two isotropic materials such as metal and ceramic. The ceramic constituent of FGMs, having high temperature resistance in combination with metal, gives high toughness. Because of the above advantages, FGMs are widely used in many fields such as aerospace, nuclear, civil engineering, automotive, biomechanics, optics…With the development in manufacturing process, completing appropriate theoretical models for structural analysis is an attractive topic for researchers. Many computational models for functionally graded (FG) plates and shells are developed, and they can be classified into three main categories according to displacement field: classical plate theory, first-order shear deformation theory and higher-order shear deformation theory. A review of various methods of studying the static and dynamic behaviors of FG plates and shells is presented in works done by Birman and Byrd (2007), Jha *et al*. (2013), Swaminathan *et al*. (2015).

The classical plate theory (CPT) ignores the transverse shear deformation effect and gives accurate results for thin plates. Analytical solution for bending analysis of Kirchhoff plates are given by Apuzzo *at al.* (2015), Barretta and Luciano (2014), Chi and Chung (2006). Based on the tolerance averaging technique, Jedrysiak and Michalak (2011) analyzed dynamic and stability behaviors of thin FG plates. Yang and Shen (2001) studied dynamic response of initially stressed FG rectangular thin plates subjected to partially distributed impulsive lateral loads. A thin-plate model including the surface effects which can be used for size-dependent static and dynamic analysis of plate-like thin film structures has been proposed by Lu *et al.* (2006). Arani *et al*. analyzed nonlinear transverse vibration of an embedded piezoelectric plate reinforced with single-walled carbon nanotubes (SWCNTs).

For moderately thick plates, first-order shear deformation theories (FSDTs) are utilized. FSDTs take into account the transverse shear deformation effect, but their accuracies depend on the shear correction factor, which is difficult to compute. Closed-form solution for free vibration of Reissner-Midlin FG plates with different combinations of boundary conditions is presented by Hosseini-Hashemi *et al*. (2010, 2011). Nguyen *et al*. (2008) performed numerical analysis for the cylindrical bending of sandwich plate with functionally graded faces. By finite element method, Alieldin *et al*. (2011), Della Croceand Venini (2004), Singha *et al*. (2011) investigated the bending behavior of FG plates. Lee *et al*. (2010) analyses post buckling response of FG plates under edge compression and temperature field conditions are presented using the element-free kp-Ritz method. Shaat *et al*. (2012, 2013) developed ananalytical solution and finite element model for continuum incorporating surface energy to study the behavior of ultra-thin functionally graded (FG) Mindlin plates. For microelectromechanical systems (MEMS) and nanoelectromechanical systems (NEMS), carbonnanotubes (CNTs) are widely used. Based on FSDT, Kolahchi *et al*. (2015b) carried out a nonlocal, nonlinear buckling analysis of embedded polymeric temperature-dependent microplates resting on an elastic matrix as an orthotropic temperature-

∗Corresponding author, Associate Professor
E-mail: tpnt2002@yahoo.com
[a]Ph.D.
[b]Ph.D. Student

ISSN: 1225-4568 (Print), 1598-6217 (Online)

dependent elastomeric medium. Kolahchi *et al*. (2016a, 2016b) presented the temperature-dependent nonlinear dynamic stability of functionally graded CNT reinforced visco-plates resting on orthotropic elastomeric medium and the dynamic stability response of an embedded piezoelectric nanoplate made of polyvinylidene fluoride.

To avoid using the shear correction factor, higher order shear deformation theories (HSDTs) are proposed. Using Navier's solutions and finite element models based on third order shear deformation theory, Reddy (2000) presented theoretical formulation for static and dynamic analysis of rectangular FG plates. Baseri *et al*. (2016) presented an analytical solution for buckling of embedded laminated plates resting on elastic foundation using Reddy's HSDT. Lü *et al.* (2009) developed a generalized and refined theory for functionally graded ultra-thin films including the surface effects. Using refined trigonometric shear deformation theory, Tounsi *et al*. (2013) studied the thermo elastic bending of functionally graded sandwich plate. Kolahchi *et al*. (2015a) investigated bending analysis of functionally graded (FG) nano-plates based on a new sinusoidal shear deformation theory. Yahia *et al*. (2015) investigated wave propagation in functionally graded plates with porosities using various higher-order shear deformation plate theories.The displacement field with five unknowns accounts for the thermo-mechanical coupling, time dependency, and the von Kármán type geometric non-linearity. Gulshan Taj *et al*. (2013) also utilized Reddy's third order shear deformation theory to analyze the static behavior of FG plates by applying finite element method. Using higher order shear deformation theory (11 unknowns) and finite element models, Talha and Singh (2010) studied free vibration and static analysis of FG plates. A higher order shear and normal deformation theory with 12 unknowns is used by Jha *et al*. to determine the natural frequency of FG plates (Jha *et al*. 2012). Navier's solution technique employing double Fourier series is used to give analytical solution. Swaminathan and Naveenkumar (2014) presented analytical formulations and solutions for the stability analysis of simply supported FG plates by various shear deformation theories, one of which is with twelve displacement's unknowns.

To describe the wrapping throughout the thickness of the plate during rotation due to transverse shear, Touratier (1991) proposed employing the sine function. Later, Zenkour (2005a, 2005b, 2006, 2009) used Touratier's sinusoidal shear deformation theory to investigate the mechanical behavior of FG plates. Analytical solutions for bending, buckling and free vibration analyses are presented in his work. Most of the above mentioned HSDTs require additional computation efforts due to the additional unknowns introduced to them (usually nine, eleven or thirteen unknowns depending on the particular theory).

In the following work, a new higher order displacement field based on twelve unknowns higher order shear deformation theory is developed. The new form is dictated by the satisfaction of vanishing transverse shear stress at the top and bottom surfaces of plate. By this approach, the number of displacement unknowns are reduce from twelve to eight, thereby saving computational time and optimizing the storage capacity of computers. The accuracy of the present theory is verified by comparing with previous studies.

2. Kınematıcs

The full higher order displacement field is given in the following form

$$\begin{aligned} u(x,y,z) &= u_0(x,y) + z\theta_x(x,y) + z^2 u_0^*(x,y) + z^3\theta_x^*(x,y);\\ v(x,y,z) &= v_0(x,y) + z\theta_y(x,y) + z^2 v_0^*(x,y) + z^3\theta_y^*(x,y);\\ w(x,y,z) &= w_0(x,y) + z\theta_z(x,y) + z^2 w_0^*(x,y) + z^3\theta_z^*(x,y). \end{aligned} \quad (1)$$

where u,v,w denote the displacements of a point along the (x,y,z) coordinates; u_0,v_0,w_0 are corresponding displacements of a point on the midplane; θ_x, θ_y and θ_z are the rotations of the line segment normal to the midplane about the y-axis, x-axis and z-axis, respectively. The functions $u_0^*, v_0^*, w_0^*, \theta_x^*, \theta_y^*$ and θ_z^* are the higher order terms in the Taylor series expansion defined in the mid-plane.

For bending plates, the transverse shear stresses σ_{xz}, σ_{yz} must be vanished at the top and bottom surfaces. These conditions lead to the requirement that the corresponding transverse strains on these surfaces be zero. From $\gamma_{xz}\left(x,y,\pm\frac{h}{2}\right) = \gamma_{yz}\left(x,y,\pm\frac{h}{2}\right) = 0$, we obtain

$$\begin{aligned} u_0^* &= -\frac{1}{2}\theta_{z,x} - \frac{h^2}{8}\theta_{z,x}^*; \theta_x^* = -\frac{4}{3h^2}\left(\theta_x + w_{0,x}\right) - \frac{1}{3}w_{0,x}^*;\\ v_0^* &= -\frac{1}{2}\theta_{z,y} - \frac{h^2}{8}\theta_{z,y}^*; \theta_y^* = -\frac{4}{3h^2}\left(\theta_y + w_{0,y}\right) - \frac{1}{3}w_{0,y}^*. \end{aligned} \quad (2)$$

The displacement field (1) becomes:

$$\begin{aligned} u &= u_0 + z\theta_x - \frac{z^2}{2}\left(\theta_{z,x} + c_1\theta_{z,x}^*\right) - \frac{z^3}{3}\left[c_2\left(\theta_x + w_{0,x}\right) + w_{0,x}^*\right];\\ v &= v_0 + z\theta_y - \frac{z^2}{2}\left(\theta_{z,y} + c_1\theta_{z,y}^*\right) - \frac{z^3}{3}\left[c_2\left(\theta_y + w_{0,y}\right) + w_{0,y}^*\right];\\ w &= w_0 + z\theta_z + z^2 w_0^* + z^3\theta_z^*. \end{aligned} \quad (3)$$

with: $c_1 = \frac{h^2}{4}; c_2 = \frac{4}{h^2}$.

The strain components and strain displacements relationships can be expressed as

$$\begin{aligned} &\varepsilon_x = \varepsilon_x^0 + z\kappa_x^0 + z^2\varepsilon_x^* + z^3\kappa_x^*;\\ &\varepsilon_y = \varepsilon_y^0 + z\kappa_y^0 + z^2\varepsilon_y^* + z^3\kappa_y^*; \varepsilon_z = \varepsilon_z^0 + z\kappa_z^0 + z^2\varepsilon_z^*;\\ &\gamma_{xy} = \varepsilon_{xy}^0 + z\kappa_y^0 + z^2\varepsilon_{xy}^* + z^3\kappa_{xy}^*;\\ &\gamma_{xz} = \gamma_{xz}^0 + z\kappa_{xz}^0 + z^2\gamma_{xz}^* + z^3\kappa_{xz}^*;\\ &\gamma_{yz} = \gamma_{yz}^0 + z\kappa_{yz}^0 + z^2\gamma_{yz}^* + z^3\kappa_{yz}^*. \end{aligned} \quad (4)$$

where

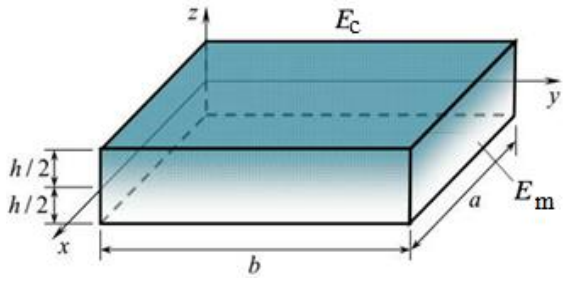

Fig. 1 Geometry of FG plate with positive set of reference axes

$$\begin{aligned}
&\left\{\varepsilon_x^0,\varepsilon_y^0,\varepsilon_z^0,\gamma_{xy}^0\right\}=\left\{u_{0,x},v_{0,y},\theta_z,u_{0,y}+v_{0,x}\right\};\\
&\left\{\kappa_x^0,\kappa_y^0,\kappa_z^0,\kappa_{xy}^0\right\}=\left\{\theta_{x,x},\theta_{y,y},2w_0^*,\theta_{x,y}+\theta_{y,x}\right\};\\
&\left\{\varepsilon_x^*,\varepsilon_y^*,\varepsilon_z^*,\gamma_{xy}^*\right\}=\left\{-\frac{1}{2}\left(\theta_{z,xx}+c_1\theta_{z,xx}^*\right),-\frac{1}{2}\left(\theta_{z,yy}+c_1\theta_{z,yy}^*\right),\right.\\
&\left.3\theta_z^*,-\left(\theta_{z,xy}+c_1\theta_{z,xy}^*\right)\right\};\left\{\gamma_{xz}^0,\gamma_{yz}^0\right\}=\left\{w_{0,x}+\theta_x,w_{0,y}+\theta_y\right\};\\
&\left\{\kappa_{xz}^0,\kappa_{yz}^0\right\}=\left\{-c_1\theta_{z,x}^*,-c_1\theta_{z,y}^*\right\};\left\{\gamma_{xz}^*,\gamma_{yz}^*\right\}=\\
&\left\{-c_2\left(w_{0,x}+\theta_x\right),-c_2\left(w_{0,y}+\theta_y\right)\right\};\left\{\kappa_{xz}^*,\kappa_{yz}^*\right\}=\left\{\theta_{z,x}^*,\theta_{z,y}^*\right\}.
\end{aligned}\tag{5}$$

In the above formulas, a comma followed by *x* or *y* denotes differentiation with respect to the coordinates *x* or *y* respectively.

3. Constitutive equation

Consider a linearly elastic rectangular simply supported FG plate of uniform thickness h as shown in Fig. 1. The Poisson's ratio *v* is assumed to be constant across the plate thickness. The Young's modulus of the FG plate is assumed to follow the power law distribution in the thickness direction, and expressed as

$$E(z)=E_m+\left(E_c-E_m\right)\left(\frac{z}{h}+\frac{1}{2}\right)^p \tag{6}$$

here subscript *c* refers to the ceramic material and subscript *m* refers to the metal material of the FG plate. It is clear from the expression that the top surface ($z=h/2$) of the FG plate is ceramic-rich and the bottom ($z=-h/2$) is metal-rich in constituents.

The stress-strain relationship for the FG plate can be written as

$$\begin{Bmatrix}\sigma_x\\ \sigma_y\\ \sigma_z\\ \sigma_{xy}\\ \sigma_{xz}\\ \sigma_{yz}\end{Bmatrix}=\begin{bmatrix}Q_{11}&Q_{12}&Q_{13}&0&0&0\\ Q_{21}&Q_{22}&Q_{23}&0&0&0\\ Q_{31}&Q_{32}&Q_{33}&0&0&0\\ 0&0&0&Q_{44}&0&0\\ 0&0&0&0&Q_{55}&0\\ 0&0&0&0&0&Q_{66}\end{bmatrix}\begin{Bmatrix}\varepsilon_x\\ \varepsilon_y\\ \varepsilon_z\\ \gamma_{xy}\\ \gamma_{xz}\\ \gamma_{yz}\end{Bmatrix} \tag{7}$$

in which (σ_x, σ_y, σ_z, σ_{xz}, σ_{yz}, σ_{xy}) are the stresses, and (ε_x, ε_y, ε_z, γ_{xz}, γ_{yz}, γ_{xy}) are the strains with respect to axes *x*, *y*, *z*. The elements of stiffness matrix Q_{ij} are defined as follows

$$\begin{aligned}
&Q_{11}=Q_{22}=Q_{33}=\frac{(1-\nu)E}{(1+\nu)(1-2\nu)};\\
&Q_{12}=Q_{23}=Q_{13}=\frac{\nu E}{(1+\nu)(1-2\nu)}=Q_{21}=Q_{32}=Q_{31};\\
&Q_{44}=Q_{55}=Q_{66}=\frac{E}{2(1+\nu)}.
\end{aligned}\tag{8}$$

4. Equilibrium equations

The principle of virtual displacement when applied to the plate can be written in analytical form as (9)

$$\begin{aligned}
0=&\int_A\int_{-h/2}^{h/2}\left(\sigma_x\delta\varepsilon_x+\sigma_y\delta\varepsilon_y+\sigma_z\delta\varepsilon_z+\sigma_{xy}\delta\gamma_{xy}+\sigma_{xz}\delta\gamma_{xz}+\right.\\
&\left.\sigma_{yz}\delta\gamma_{yz}\right)dA\,dz-\int_A q_z^+\delta w^+dA=\int_A\left\{N_x\delta u_{0,x}+M_x\delta\theta_{x,x}\right.\\
&-\frac{N_x^*}{2}\left(\delta\theta_{z,xx}+c_1\delta\theta_{z,xx}^*\right)-\frac{M_x^*}{3}\left(c_2\left(\delta\theta_{x,x}+\delta w_{0,xx}\right)+\delta w_{0,xx}^*\right)\\
&+N_y\delta v_{0,y}+M_y\delta\theta_{y,y}-\frac{N_y^*}{2}\left(\delta\theta_{z,yy}+c_1\delta\theta_{z,yy}^*\right)-\\
&-\frac{M_y^*}{3}\left(c_2\left(\delta\theta_{y,y}+\delta w_{0,yy}\right)+\delta w_{0,yy}^*\right)+N_z\delta\theta_z+2M_z\delta w_0^*\\
&+3N_z^*\delta\theta_z^*+N_{xy}\left(\delta u_{0,y}+\delta v_{0,x}\right)+M_{xy}\left(\delta\theta_{x,y}+\delta\theta_{y,x}\right)\\
&-N_{xy}^*\left(\delta\theta_{z,xy}+c_1\delta\theta_{z,xy}^*\right)-\frac{M_{xy}^*}{3}\left(c_2\left(\delta\theta_{x,y}+\delta\theta_{y,x}+2\delta w_{0,xy}\right)+\right.\\
&2\delta w_{0,xy}^*\Big)+Q_x\left(\delta\theta_x+\delta w_{0,x}\right)-S_xc_1\delta\theta_{z,x}^*-Q_x^*c_2\left(\delta\theta_x+\delta w_{0,x}\right)\\
&+S_x^*\delta\theta_{z,x}^*+Q_y\left(\delta\theta_y+\delta w_{0,y}\right)-S_yc_1\theta_{z,y}^*-Q_y^*c_2\left(\delta\theta_y+\delta w_{0,y}\right)+\\
&\left.\left.S_y^*\delta\theta_{z,y}^*+q_z^+\left(\delta w_0+\frac{h}{2}\delta\theta_z+\frac{h^2}{4}\delta w_0^*+\frac{h^3}{8}\delta\theta_z^*\right)\right\}dA
\end{aligned}\tag{9}$$

where symbol δ denotes the variational operator, q_z^+ the transverse load applied at the top surface of the plate, and (10)

$$\begin{aligned}
&\begin{Bmatrix}N_x\\ N_y\\ N_z\\ N_{xy}\end{Bmatrix}=\int_{-h/2}^{h/2}\begin{Bmatrix}\sigma_x\\ \sigma_y\\ \sigma_z\\ \sigma_{xy}\end{Bmatrix}dz;\begin{Bmatrix}M_x\\ M_y\\ M_z\\ M_{xy}\end{Bmatrix}=\\
&\int_{-h/2}^{h/2}\begin{Bmatrix}\sigma_x\\ \sigma_y\\ \sigma_z\\ \sigma_{xy}\end{Bmatrix}z\,dz;\begin{Bmatrix}N_x^*\\ N_y^*\\ N_z^*\\ N_{xy}^*\end{Bmatrix}=\int_{-h/2}^{h/2}\begin{Bmatrix}\sigma_x\\ \sigma_y\\ \sigma_z\\ \sigma_{xy}\end{Bmatrix}z^2dz;\\
&\begin{Bmatrix}M_x^*\\ M_y^*\\ M_{xy}^*\end{Bmatrix}=\int_{-h/2}^{h/2}\begin{Bmatrix}\sigma_x\\ \sigma_y\\ \sigma_{xy}\end{Bmatrix}z^3dz;\begin{Bmatrix}Q_x\\ Q_y\end{Bmatrix}=
\end{aligned}$$

$$\int_{-h/2}^{h/2}\begin{Bmatrix}\sigma_{xz}\\ \sigma_{yz}\end{Bmatrix}dz;\begin{Bmatrix}S_x\\ S_y\end{Bmatrix}=\int_{-h/2}^{h/2}\begin{Bmatrix}\sigma_{xz}\\ \sigma_{yz}\end{Bmatrix}z\,dz;$$

$$\begin{Bmatrix}Q_x^*\\ Q_y^*\end{Bmatrix}=\int_{-h/2}^{h/2}\begin{Bmatrix}\sigma_{xz}\\ \sigma_{yz}\end{Bmatrix}z^2dz;\begin{Bmatrix}S_x^*\\ S_y^*\end{Bmatrix}=\int_{-h/2}^{h/2}\begin{Bmatrix}\sigma_{xz}\\ \sigma_{yz}\end{Bmatrix}z^3dz. \tag{10}$$

From Eqs. (4), (7), and (10) we obtain

$$\begin{Bmatrix}N_x\\ N_y\\ N_z\\ N_{xy}\\ M_x\\ M_y\\ M_z\\ M_{xy}\\ N_x^*\\ N_y^*\\ N_z^*\\ N_{xy}^*\\ M_x^*\\ M_y^*\\ M_{xy}^*\end{Bmatrix}=\begin{bmatrix}A_{11}&A_{12}&A_{13}&0&B_{11}&B_{12}&B_{13}\\ A_{21}&A_{22}&A_{23}&0&B_{21}&B_{22}&B_{23}\\ A_{31}&A_{32}&A_{33}&0&B_{31}&B_{32}&B_{33}\\ 0&0&0&A_{44}&0&0&0\\ B_{11}&B_{12}&B_{13}&0&C_{11}&C_{12}&C_{13}\\ B_{21}&B_{22}&B_{23}&0&C_{21}&C_{22}&C_{23}\\ B_{31}&B_{32}&B_{33}&0&C_{31}&C_{32}&C_{33}\\ 0&0&0&B_{44}&0&0&0\\ C_{11}&C_{12}&C_{13}&0&D_{11}&D_{12}&D_{13}\\ C_{21}&C_{22}&C_{23}&0&D_{21}&D_{22}&D_{23}\\ C_{31}&C_{32}&C_{33}&0&D_{31}&D_{32}&D_{33}\\ 0&0&0&C_{44}&0&0&0\\ D_{11}&D_{12}&D_{13}&0&E_{11}&E_{12}&E_{13}\\ D_{21}&D_{22}&D_{23}&0&E_{21}&E_{22}&E_{23}\\ 0&0&0&D_{44}&0&0&0\end{bmatrix}$$

$$\begin{bmatrix}0&C_{11}&C_{12}&C_{13}&0&D_{11}&D_{12}&0\\ 0&C_{21}&C_{22}&C_{23}&0&D_{21}&C_{22}&0\\ 0&C_{31}&C_{32}&C_{33}&0&D_{31}&D_{32}&0\\ B_{44}&0&0&0&C_{44}&0&0&D_{44}\\ 0&D_{11}&D_{12}&D_{13}&0&E_{11}&E_{12}&0\\ 0&D_{21}&D_{22}&D_{23}&0&E_{21}&E_{22}&0\\ 0&D_{31}&D_{32}&D_{33}&0&E_{31}&E_{32}&0\\ C_{44}&0&0&0&D_{44}&0&0&E_{44}\\ 0&E_{11}&E_{12}&E_{13}&0&F_{11}&F_{12}&0\\ 0&E_{21}&E_{22}&E_{23}&0&F_{21}&F_{22}&0\\ 0&E_{31}&E_{32}&E_{33}&0&F_{31}&F_{32}&0\\ D_{44}&0&0&0&E_{44}&0&0&F_{44}\\ 0&F_{11}&F_{12}&F_{13}&0&G_{11}&G_{12}&0\\ 0&F_{21}&F_{22}&F_{23}&0&G_{21}&G_{22}&0\\ E_{44}&0&0&0&F_{44}&0&0&G_{44}\end{bmatrix}\begin{Bmatrix}\varepsilon_x^0\\ \varepsilon_y^0\\ \varepsilon_z^0\\ \gamma_{xy}^0\\ \kappa_x^0\\ \kappa_y^0\\ \kappa_z^0\\ \kappa_{xy}^0\\ \varepsilon_x^*\\ \varepsilon_y^*\\ \varepsilon_z^*\\ \gamma_{xy}^*\\ \kappa_x^*\\ \kappa_y^*\\ \kappa_{xy}^*\end{Bmatrix}; \tag{11a}$$

$$\begin{Bmatrix}Q_x\\ Q_y\\ S_x\\ S_y\\ Q_x^*\\ Q_y^*\\ S_x^*\\ S_y^*\end{Bmatrix}=\begin{bmatrix}A_{55}&0&B_{55}&0&C_{55}&0&D_{55}&0\\ 0&A_{66}&0&B_{66}&0&C_{66}&0&D_{66}\\ B_{55}&0&C_{55}&0&D_{55}&0&E_{55}&0\\ 0&B_{66}&0&C_{66}&0&D_{66}&0&E_{66}\\ C_{55}&0&D_{55}&0&E_{55}&0&F_{55}&0\\ 0&C_{66}&0&D_{66}&0&E_{66}&0&F_{66}\\ D_{55}&0&E_{55}&0&F_{55}&0&G_{55}&0\\ 0&D_{66}&0&E_{66}&0&F_{66}&0&G_{66}\end{bmatrix}\begin{Bmatrix}\gamma_{xz}^0\\ \gamma_{yz}^0\\ \kappa_{xz}^0\\ \kappa_{yz}^0\\ \gamma_{xz}^*\\ \gamma_{yz}^*\\ \kappa_{xz}^*\\ \kappa_{yz}^*\end{Bmatrix}. \tag{11b}$$

where A_{ij}, B_{ij}, C_{ij}, D_{ij}, E_{ij}, F_{ij}, G_{ij} are the plate stiffness coeficients, defined by

$$\left(A_{ij},B_{ij},C_{ij},D_{ij},E_{ij},F_{ij},G_{ij}\right)=$$

$$\int_{-h/2}^{h/2}Q_{ij}\left(1,z,z^2,z^3,z^4,z^5,z^6\right)dz;\qquad (i,j=1,2,3,4,5,6)$$

Integrating the expression in equation (9) by parts and setting the coefficients of $\delta u_0,\delta v_0,\delta w_0,\delta\theta_x,\delta\theta_y,\delta\theta_z,\delta w_0^*,\delta\theta_z^*$ to zero separately, we obtain the following equilibrium equations

$$\begin{aligned}
&\delta u_0: N_{x,x}+N_{xy,y}=0;\\
&\delta v_0: N_{y,y}+N_{xy,x}=0;\\
&\delta w_0: \frac{c_2}{3}\left(M_{x,xx}^*+2M_{xy,xy}^*+M_{y,yy}^*\right)-\\
&c_2\left(Q_{x,x}^*+Q_{y,y}^*\right)+\left(Q_{x,x}+Q_{y,y}\right)+q_z^+=0;\\
&\delta\theta_x: \frac{c_2}{3}\left(M_{x,x}^*+M_{xy,y}^*\right)-\left(M_{x,x}+M_{xy,y}\right)-c_2Q_x^*+Q_x=0;\\
&\delta\theta_y: \frac{c_2}{3}\left(M_{xy,x}^*+M_{y,y}^*\right)-\left(M_{xy,x}+M_{y,y}\right)-c_2Q_y^*+Q_y=0;\\
&\delta\theta_z: \frac{1}{2}\left(N_{x,xx}^*+2N_{xy,xy}^*+N_{y,yy}^*\right)-N_z+\frac{h}{2}q_z^+=0;\\
&\delta w_0^*: \frac{1}{3}\left(M_{x,xx}^*+2M_{xy,xy}^*+M_{y,yy}^*\right)-2M_z+\frac{h^2}{4}q_z^+=0;\\
&\delta\theta_z^*: \frac{c_1}{2}\left(N_{x,xx}^*+2N_{xy,xy}^*+N_{y,yy}^*\right)-3N_z^*+\left(S_{x,x}^*+S_{y,y}^*\right)-c_1
\end{aligned} \tag{12}$$

5. Navier's solution

Consider a simply supported rectangular FG plate subjected to transverse distributed loading. The associated simply supported boundary conditions are as follows:

At edge x=0 and x=a:

$$\begin{aligned}&v_0=0;w_0=0;\theta_y=0;\theta_z=0;\\&w_0^*=0;\theta_z^*=0;M_x=0;M_x^*=0\end{aligned} \tag{13a}$$

At edge y=0 and y=b:

$$\begin{aligned}&u_0=0;w_0=0;\theta_x=0;\theta_z=0;\\&w_0^*=0;\theta_z^*=0;M_y=0;M_y^*=0\end{aligned} \tag{13b}$$

Following Navier's solution procedure the displacement variables satisfying the simply supported boundary condition are written in the form (14)

$$\begin{aligned}
u_0&=\sum_{m=1}^{\infty}\sum_{n=1}^{\infty}u_{0mn}\cos\alpha x\sin\beta y;\\
v_0&=\sum_{m=1}^{\infty}\sum_{n=1}^{\infty}v_{0mn}\sin\alpha x\cos\beta y;\\
w_0&=\sum_{m=1}^{\infty}\sum_{n=1}^{\infty}w_{0mn}\sin\alpha x\sin\beta y;\\
\theta_x&=\sum_{m=1}^{\infty}\sum_{n=1}^{\infty}\theta_{xmn}\cos\alpha x\sin\beta y;
\end{aligned}$$

$$\begin{aligned}
\theta_y &= \sum_{m=1}^{\infty}\sum_{n=1}^{\infty}\theta_{ymn}\sin\alpha x\cos\beta y;\\
\theta_z &= \sum_{m=1}^{\infty}\sum_{n=1}^{\infty}\theta_{zmn}\sin\alpha x\sin\beta y;\\
w_0^* &= \sum_{m=1}^{\infty}\sum_{n=1}^{\infty}w_{0mn}^*\sin\alpha x\sin\beta y;\\
\theta_z^* &= \sum_{m=1}^{\infty}\sum_{n=1}^{\infty}\theta_{zmn}^*\sin\alpha x\sin\beta y.
\end{aligned} \tag{14}$$

where $\alpha = \dfrac{m\pi}{a};\ \beta = \dfrac{n\pi}{b}.$

The applied transverse load $q_z^+(x,y)$ is also expanded in double-Fourier sine series

$$q_z^+(x,y) = \sum_{m=1}^{\infty}\sum_{n=1}^{\infty}q_{mn}\sin\alpha x\sin\beta y \tag{15a}$$

The coefficients q_{mn} are given below for any typical loads

$$q_{mn} = \frac{4}{ab}\int_0^a\int_0^b q_z^+(x,y)\sin\alpha x\sin\beta y\,dx\,dy \tag{15b}$$

for uniformly distributed load: $q_{mn} = \dfrac{16q_0}{\pi^2 mn}$;

for sinusoidally distributed load: $q_{mn}=q_0$

Substituting Eqs. (14) and (15) in to Eq. (8) and collecting the coefficients, we obtain an 8×8 system of equations

$$\begin{bmatrix}
s_{11} & s_{12} & s_{13} & s_{14} & s_{15} & s_{16} & s_{17} & s_{18}\\
s_{21} & s_{22} & s_{23} & s_{24} & s_{25} & s_{26} & s_{27} & s_{28}\\
s_{31} & s_{32} & s_{33} & s_{34} & s_{35} & s_{36} & s_{37} & s_{38}\\
s_{41} & s_{42} & s_{43} & s_{44} & s_{45} & s_{46} & s_{47} & s_{48}\\
s_{51} & s_{52} & s_{53} & s_{54} & s_{55} & s_{56} & s_{57} & s_{58}\\
s_{61} & s_{62} & s_{63} & s_{64} & s_{65} & s_{66} & s_{67} & s_{68}\\
s_{71} & s_{72} & s_{73} & s_{74} & s_{75} & s_{76} & s_{77} & s_{78}\\
s_{81} & s_{82} & s_{83} & s_{84} & s_{85} & s_{86} & s_{7} & s_{88}
\end{bmatrix}
\begin{Bmatrix}
u_{0mn}\\ v_{0mn}\\ w_{0mn}\\ \theta_{xmn}\\ \theta_{ymn}\\ \theta_{zmn}\\ w_{0mn}^*\\ \theta_{zmn}^*
\end{Bmatrix} =
\begin{Bmatrix}
0\\ 0\\ q_{mn}\\ 0\\ 0\\ \dfrac{h}{2}q_{mn}\\ \dfrac{h^2}{4}q_{mn}\\ \dfrac{h^3}{8}q_{mn}
\end{Bmatrix} \tag{16}$$

for any fixed values of m and n. The elements s_{ij} of the coefficient matrix [s] are given in Appendix A.

The analytical solutions can be obtained from Eq. (16).

6. Results and discussion

A Matlab codes are built based on the present theoretical formulation for bending analysis of simply (diaphragm) supported FG plates. The material properties of FG plates are presented in Table 1. The deflection, in-plane and transverse stresses are presented in the following dimensionless form for convenience

Table 1 Material properties of FG plate

Properties	Metal	Ceramic
	Aluminum (Al)	Alumina(Al_2O_3)
E (GPa)	70	380
v	0.3	0.3

$$\begin{aligned}
&\bar{w} = \frac{10E_c h^3}{q_0 a^4}w\left(\frac{a}{2},\frac{b}{2},0\right);\ \bar{\sigma}_x(z) = \frac{h}{q_0 a}\sigma_x\left(\frac{a}{2},\frac{b}{2},z\right);\\
&\bar{\sigma}_y(z) = \frac{h}{q_0 a}\sigma_y\left(\frac{a}{2},\frac{b}{2},z\right);\ \bar{\sigma}_{xy}(z) = \frac{h}{q_0 a}\sigma_{xy}(0,0,z);\\
&\bar{\sigma}_{xz}(z) = \frac{h}{q_0 a}\sigma_{xz}\left(0,\frac{b}{2},z\right);\ \bar{\sigma}_{yz}(z) = \frac{h}{q_0 a}\sigma_{yz}\left(\frac{a}{2},0,z\right).
\end{aligned} \tag{17}$$

In order to validate the accuracy, Example 1 gives the numerical results using present eight-unknown HSDT. Obtained results are compared with other shear deformation theory available in literature. In the next examples, the various numerical results are presented to investigate the effects of power-law index, aspect ratio, side-to-thickness ratio on the bending behavior of FG plates. Those numerical results also reinforce the efficiency of present eight-unknown HSDT in comparing with other shear deformation theories. The following models of shear deformation theories are used in this section

HSDT-12:
$$\begin{aligned}
u &= u_0 + z\theta_x + z^2u_0^* + z^3\theta_x^*;\\
v &= v_0 + z\theta_y + z^2v_0^* + z^3\theta_y^*;\\
w &= w_0 + z\theta_z + z^2w_0^* + z^3\theta_z^*.
\end{aligned}$$

HSDT-9:
$$\begin{aligned}
u &= u_0 + z\theta_x + z^2u_0^* + z^3\theta_x^*;\\
v &= v_0 + z\theta_y + z^2v_0^* + z^3\theta_y^*;\ w = w_0.
\end{aligned}$$

HSDT-5:
$$\begin{aligned}
u &= u_0 + z\theta_x - z^3\frac{4}{3h^2}\left(\theta_x + \partial w_0/\partial x\right);\\
v &= v_0 + z\theta_y - z^3\frac{4}{3h^2}\left(\theta_y + \partial w_0/\partial y\right);\\
w &= w_0.
\end{aligned}$$

Quasi-3D HSDT:
$$\begin{aligned}
u &= u_0 + z\theta_x + z^3\theta_x^*;\\
v &= v_0 + z\theta_y + z^3\theta_y^*;\\
w &= w_0 + z\theta_z + z^2w_0^*.
\end{aligned}$$

Example 1 - Verification: A moderately thick (a/h=10) simply supported square FG plate under uniformly distributed transverse load is considered. Table 2 presents the dimensionless deflection and stresses for different values of power-law index p. The numerical results using present eight-unknown HSDT are compared with those using five-unknown Zenkour's generalized shear deformation theory (Zenkour 2006) and four-unknowns Thai's simple first-order shear deformation theory (Thai and Choi 2013). It can be seen that a good agreement is obtained for all values of power law index p. There is a more significant difference for stresses $\bar{\sigma}_{xz}, \bar{\sigma}_{yz}$ due to the neglecting of ε_z in the works of Zenkour and Thai.

The dimensionless central deflection and normal stress $\bar{\sigma}_x(h/3)$ from present higher-order shear deformation

theory are given in Table 3. The results are those of a simply supported square FG plate with a bi-sinusoidal transverse mechanical load applied at the top plate surface. Three side-to-thickness ratios (a/h=4, 10 and 100) and five power-law indexes (p=0, 0.5, 1, 4 and 10) are considered. The results, which account for ε_z are compared with those from Neves *et al*. (2013) using a quasi-3D higher-order shear deformation theory done by meshless techniques, those from Neves *et al*. (2012) using a quasi-3D sinusoidal shear deformation theory, and those from Carrera *et al*. (2008, 2011). From Table 3, it could be concluded that the present HSDT presents very close results to quasi-3D higher-order shear deformation theory.

Fig. 2 plots the through-the-thickness distributions of the dimensionless in-plane stresses and transverse shear stresses at the specified positions of square FG plate under uniform load with power-law index p=2. It is shown that the present results are in a good agreement with those predicted using nine-unknown (HSDT-9) and twelve-unknown (HSDT-12) higher order shear deformation theories for the in-plane stresses $\bar{\sigma}_x\left(\frac{a}{2},\frac{b}{2},z\right)$, $\bar{\sigma}_{xy}(0,0,z)$. Note that the present eight-unknown HSDT and HSDT-12 take into account the thickness stretching effect $(\varepsilon_z \neq 0)$, but HSDT-9 neglects the thickness stretching effect. Present HSDT presents better representation of the transverse shear stresses $\bar{\sigma}_{xz},\bar{\sigma}_{yz}$, they are zero at the top and bottom of the FG plates; while according to the HSDT-9 and HSDT-12 the vanishing of transverse stresses at the top and bottom surfaces is not satisfied.

Example 2. A moderately thick simply supported square FG plate (a = b = 10h) under uniform load is considered. Table 4 contains dimensionless deflection and stresses for different values of power-law index p. Figure 3 shows the variation of dimensionless deflection $\bar{w}$, in-plane stresses $\bar{\sigma}_x,\bar{\sigma}_{xy}$, and transverse stress $\bar{\sigma}_{xz}$ versus the power law

Table 2 Dimensionless deflection and stresses of square plates under uniform loads (a/h=10)

p	Method	$\bar{w}$	$\bar{\sigma}_x(h/2)$	$\bar{\sigma}_y(h/3)$	$\bar{\sigma}_{xy}(-h/3)$	$\bar{\sigma}_{xz}(0)$	$\bar{\sigma}_{yz}(h/6)$
	Zenkour (2006)	0.4665	2.8932	1.9103	1.2850	0.4429	0.5114
0	Thai and Choi (2013)	0.4666	2.8732	1.9155	1.2990	0.4004	0.4004
	Present	**0.4640**	**2.9050**	**1.9229**	**1.2855**	**0.4881**	**0.4351**
	Zenkour (2006)	0.9287	4.4745	2.1692	1.1143	0.5446	0.5114
1	Thai and Choi (2013)	0.9288	4.4407	2.1767	1.1218	0.4923	0.4004
	Present	**0.9266**	**4.4851**	**2.1819**	**1.1113**	**0.4871**	**0.5349**
	Zenkour (2006)	1.1940	5.2296	2.0338	0.9907	0.5734	0.4700
2	Thai and Choi (2013)	1.1909	5.1853	2.0441	0.9998	0.4799	0.3407
	Present	**1.1925**	**5.2394**	**2.0466**	**0.9909**	**0.4457**	**0.5610**
	Zenkour (2006)	1.3200	5.6108	1.8593	1.0047	0.5629	0.4367
3	Thai and Choi (2013)	1.3123	5.5576	1.8719	1.0160	0.4393	0.2952
	Present	**1.3187**	**5.6173**	**1.8724**	**1.0074**	**0.4123**	**0.5201**
	Zenkour (2006)	1.3890	5.8915	1.7191	1.0298	0.5346	0.4204
4	Thai and Choi (2013)	1.3770	5.8316	1.7338	1.0427	0.3981	0.2711
	Present	**1.3874**	**5.8940**	**1.7331**	**1.0341**	**0.3959**	**0.5201**
	Zenkour (2006)	1.4356	6.1504	1.6104	1.0451	0.5031	0.4177
5	Thai and Choi (2013)	1.4205	6.0857	1.6252	1.0591	0.3647	0.2622
	Present	**1.4338**	**6.1493**	**1.6240**	**1.0504**	**0.3930**	**0.4893**
	Zenkour (2006)	1.4727	6.4043	1.5214	1.0536	0.4755	0.4227
6	Thai and Choi (2013)	1.4555	6.3364	1.5364	1.0683	0.3406	0.2622
	Present	**1.4706**	**6.4005**	**1.5350**	**1.0594**	**0.3979**	**0.4629**
	Zenkour (2006)	1.5049	6.6547	1.4467	1.0589	0.4543	0.4310
7	Thai and Choi (2013)	1.4867	6.5847	1.4615	1.0740	0.3245	0.2666
	Present	**1.5026**	**6.6489**	**1.4599**	**1.0649**	**0.4062**	**0.4429**
	Zenkour (2006)	1.5343	6.8999	1.3829	1.0628	0.4392	0.4399
8	Thai and Choi (2013)	1.5158	6.8287	1.3973	1.0782	0.3147	0.2730
	Present	**1.5317**	**6.8929**	**1.3958**	**1.0689**	**0.4152**	**0.4289**
	Zenkour (2006)	1.5617	7.1383	1.3283	1.0662	0.4291	0.4481
9	Thai and Choi (2013)	1.5433	7.0663	1.3422	1.0819	0.3095	0.2799
	Present	**1.5590**	**7.1306**	**1.3408**	**1.0723**	**0.4236**	**0.4197**
	Zenkour (2006)	1.5876	7.3689	1.2820	1.0694	0.4227	0.4552
10	Thai and Choi (2013)	1.5697	7.2963	1.2953	1.0853	0.3074	0.2867
	Present	**1.5847**	**7.3608**	**1.2940**	**1.0755**	**0.4310**	**0.4141**

Table 3 Dimensionless deflection and stresses of square plates under bi-sinusoidal loads

p	a/h	$\bar{\sigma}_x(h/3)$			$\bar{w}$		
		4	10	100	4	10	100
0	Neves *et al.* (2013)	0.5278	1.3176	13.161	0.3665	0.2942	0.2803
	Present	**0.5475**	**1.3252**	**13.1726**	**0.3665**	**0.2943**	**0.2804**
0.5	Neves *et al.* (2013)	0.5860	1.4680	14.673	0.5493	0.4548	0.4365
	Present	**0.6028**	**1.4713**	**14.6458**	**0.5534**	**0.4520**	**0.4325**
1	Neves *et al.* (2013)	0.5911	1.4917	14.945	0.7020	0.5868	0.5647
	Carera *et al.* (2008)	0.6221	1.5064	14.969	0.7171	0.5875	0.5625
	Carera *et al.* (2011)	0.6221	1.5064	14.969	0.7171	0.5875	0.5625
	Neves *et al.* (2012)	0.5925	1.4945	14.969	0.6997	0.5845	0.5624
	Present	**0.6114**	**1.5021**	**14.9688**	**0.7020**	**0.5875**	**0.5625**
4	Neves *et al.* (2013)	0.4330	1.1588	11.737	1.1108	0.8700	0.8240
	Carera *et al.* (2008)	0.4877	1.1971	11.923	1.1585	0.8821	0.8286
	Carera *et al.* (2011)	0.4877	1.1971	11.923	1.1585	0.8821	0.8286
	Neves *et al.* (2012)	0.4404	1.1783	11.932	1.1178	0.8750	0.8286
	Present	**0.4724**	**1.1909**	**11.9221**	**1.1517**	**0.8808**	**0.8287**
10	Neves *et al.* (2013)	0.3097	0.8462	8.6010	1.3334	0.9888	0.9227
	Carera *et al.* (2008)	0.3695	0.8965	8.9077	1.3745	1.0072	0.9361
	Carera *et al.* (2011)	0.1478	0.8965	8.9077	1.3745	1.0072	0.9361
	Neves *et al.* (2012)	0.3227	1.1783	11.932	1.3490	0.8750	0.8286
	Present	**0.3493**	**0.8885**	**8.9070**	**1.3748**	**1.0069**	**0.9362**

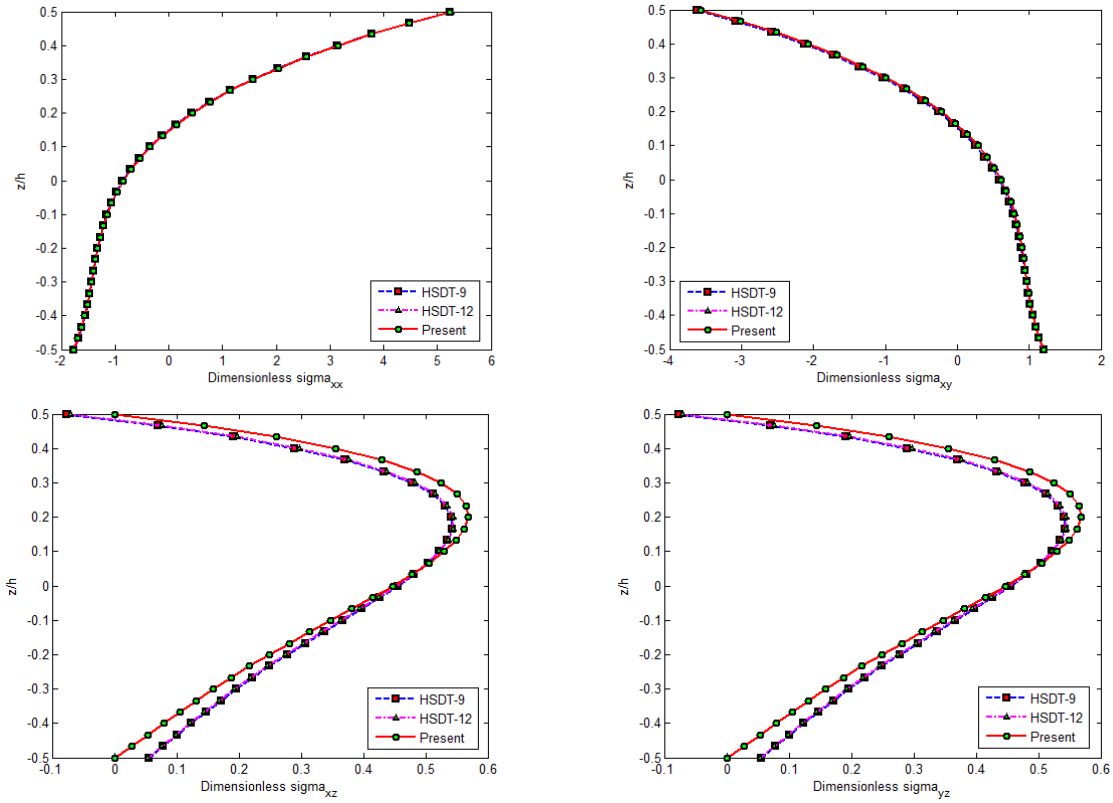

Fig. 2 Variation of dimensionless stresses through the thickness of square plates under uniform loads (a=b=10h, p=2)

index p of square plates under uniform loads. It is observed that the dimensionless deflection $\bar{w}$ and normal stress $\bar{\sigma}_x$ increase as the power law index increases. In-plane stress σ_{xy} decreases in range of p from 0 to 2, then increases with increasing power law index. Transverse stress σ_{xz}, σ_{yz} slightly changes in range of p from 0 to 1, decreases in range of p from 1 to 5, and then increases slowly with increasing power law index. Effect of HSDT is significant

Table 4 Dimensionless deflection and stresses of square plates under uniform loads (a/h=10) with different value of power-law index p

p	Method	$\bar{w}$	$\bar{\sigma}_x(h/2)$	$\bar{\sigma}_y(h/3)$	$\bar{\sigma}_{xy}(-h/3)$	$\bar{\sigma}_{xz}(0)$	$\bar{\sigma}_{yz}(h/6)$
0	FSDT	0.4666	2.8726	1.9150	1.2975	0.3927	0.3927
	HSDT-5	0.4666	2.8901	1.9105	1.2861	0.4890	0.4347
	HSDT-9	0.4666	2.8905	1.9104	1.2870	0.4877	0.4342
	HSDT-12	0.4640	2.9064	1.9226	1.2892	0.4864	0.4364
	Present	**0.4640**	**2.9050**	**1.9229**	**1.2855**	**0.4881**	**0.4351**
1	FSDT	0.9288	4.4397	2.1762	1.1205	0.3927	0.4829
	HSDT-5	0.9288	4.4694	2.1696	1.1144	0.4890	0.5345
	HSDT-9	0.9289	4.4730	2.1700	1.1135	0.4876	0.5222
	HSDT-12	0.9268	4.4881	2.1821	1.1122	0.4855	0.5236
	Present	**0.9266**	**4.4851**	**2.1819**	**1.1113**	**0.4871**	**0.5349**
3	FSDT	1.3123	5.5564	1.8715	1.0148	0.2896	0.4310
	HSDT-5	1.3197	5.6030	1.8605	1.0057	0.4144	0.5482
	HSDT-9	1.3209	5.6183	1.8596	1.0032	0.4254	0.5336
	HSDT-12	1.3199	5.6301	1.8715	1.0059	0.4231	0.5346
	Present	**1.3187**	**5.6173**	**1.8724**	**1.0074**	**0.4123**	**0.5487**
5	FSDT	1.4205	6.0843	1.6249	1.0579	0.2572	0.3577
	HSDT-5	1.4349	6.1411	1.6120	1.0466	0.3950	0.4883
	HSDT-9	1.4360	6.1573	1.6099	1.0447	0.4080	0.4861
	HSDT-12	1.4349	6.1649	1.6215	1.0494	0.4059	0.4871
	Present	**1.4338**	**6.1493**	**1.6240**	**1.0504**	**0.3930**	**0.4893**
10	FSDT	1.5696	7.2947	1.2950	1.0840	0.2812	0.3015
	HSDT-5	1.5872	7.3588	1.2834	1.0711	0.4326	0.4123
	HSDT-9	1.5875	7.3644	1.2822	1.0711	0.4415	0.4199
	HSDT-12	1.5850	7.3694	1.2921	1.0767	0.4397	0.4213
	Present	**1.5847**	**7.3608**	**1.2940**	**1.0755**	**0.4310**	**0.4141**

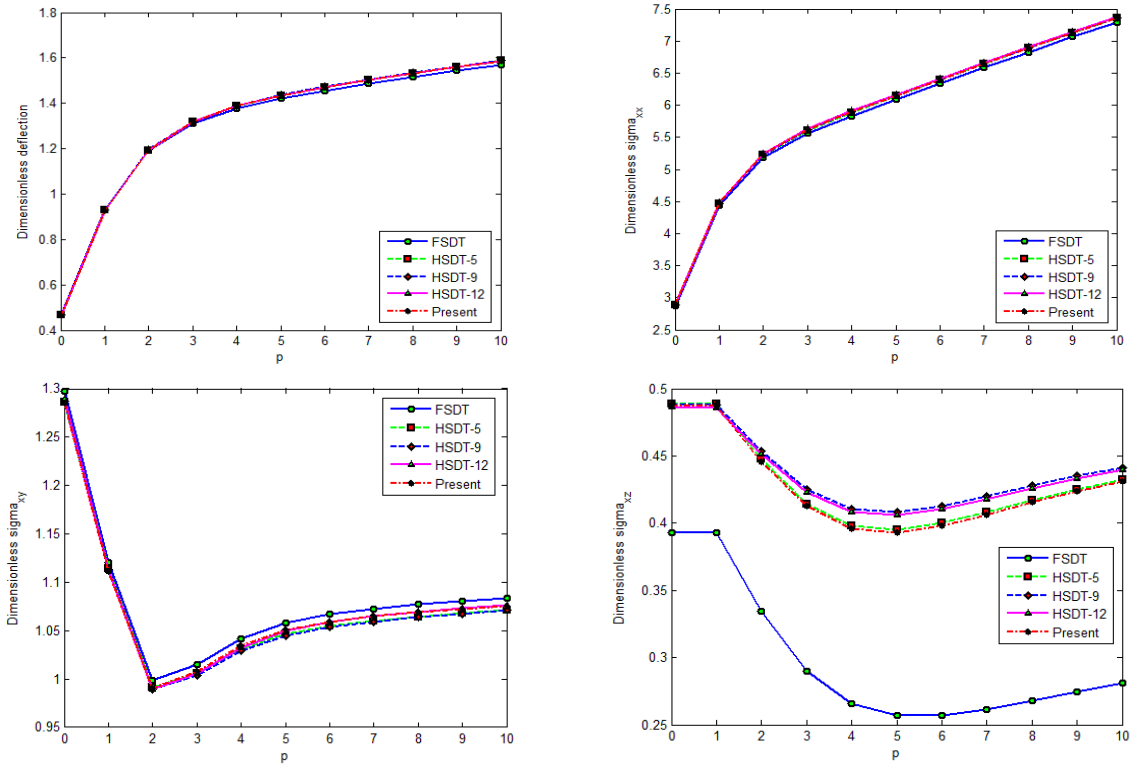

Fig. 3 Variation of dimensionless deflection $\bar{w}$, in-plane stresses $\bar{\sigma}_x, \bar{\sigma}_{xy}$, transverse stress $\bar{\sigma}_{xz}$ versus power law index p of square plates under uniform loads (a=b=10h)

Table 5 Dimensionless deflection and stresses of square plates under uniform loads (a=b, p=5) with various value of side-to-thickness a/h

a/h	Method	$\bar{w}$	$\bar{\sigma}_x(h/2)$	$\bar{\sigma}_y(h/3)$	$\bar{\sigma}_{xy}(-h/3)$	$\bar{\sigma}_{xz}(0)$	$\bar{\sigma}_{yz}(h/6)$
5	FSDT	1.6358	3.0422	0.8124	0.5289	0.2572	0.3577
	HSDT-5	1.6929	3.1578	0.7863	0.5079	0.3895	0.4815
	HSDT-9	1.6969	3.1909	0.7820	0.5066	0.4003	0.4793
	HSDT-12	1.6911	3.2097	0.8052	0.5090	0.3914	0.4796
	Present	**1.6871**	**3.1804**	**0.8103**	**0.5070**	**0.3813**	**0.4810**
10	FSDT	1.4205	6.0843	1.6249	1.0579	0.2572	0.3577
	HSDT-5	1.4349	6.1411	1.6120	1.0466	0.3950	0.4883
	HSDT-9	1.4360	6.1573	1.6099	1.0447	0.4080	0.4861
	HSDT-12	1.4349	6.1649	1.6215	1.0494	0.4059	0.4871
	Present	**1.4338**	**6.1493**	**1.6240**	**1.0504**	**0.3930**	**0.4893**
20	FSDT	1.3666	12.1686	3.2497	2.1157	0.2572	0.3577
	HSDT-5	1.3703	12.1968	3.2434	2.1099	0.3966	0.4903
	HSDT-9	1.3705	12.2044	3.2424	2.1085	0.4109	0.4885
	HSDT-12	1.3703	12.2087	3.2480	2.1127	0.4106	0.4888
	Present	**1.3700**	**12.2018**	**3.2490**	**2.1141**	**0.3963**	**0.4908**
50	FSDT	1.3516	30.4216	8.1243	5.2893	0.2572	0.3577
	HSDT-5	1.3521	30.4328	8.1217	5.2869	0.3971	0.4909
	HSDT-9	1.3522	30.4358	8.1214	5.2863	0.4118	0.4893
	HSDT-12	1.3521	30.4379	8.1235	5.2883	0.4118	0.4893
	Present	**1.3521**	**30.4353**	**8.1239**	**5.2890**	**0.3971**	**0.4910**
100	FSDT	1.3494	60.8432	16.2486	10.5785	0.2572	0.3577
	HSDT-5	1.3496	60.8488	16.2473	10.5774	0.3972	0.4910
	HSDT-9	1.3496	60.8503	16.2471	10.5770	0.4120	0.4894
	HSDT-12	1.3496	60.8514	16.2482	10.5781	0.4120	0.4894
	Present	**1.3495**	**60.8501**	**16.2484**	**10.5784**	**0.3972**	**0.4910**

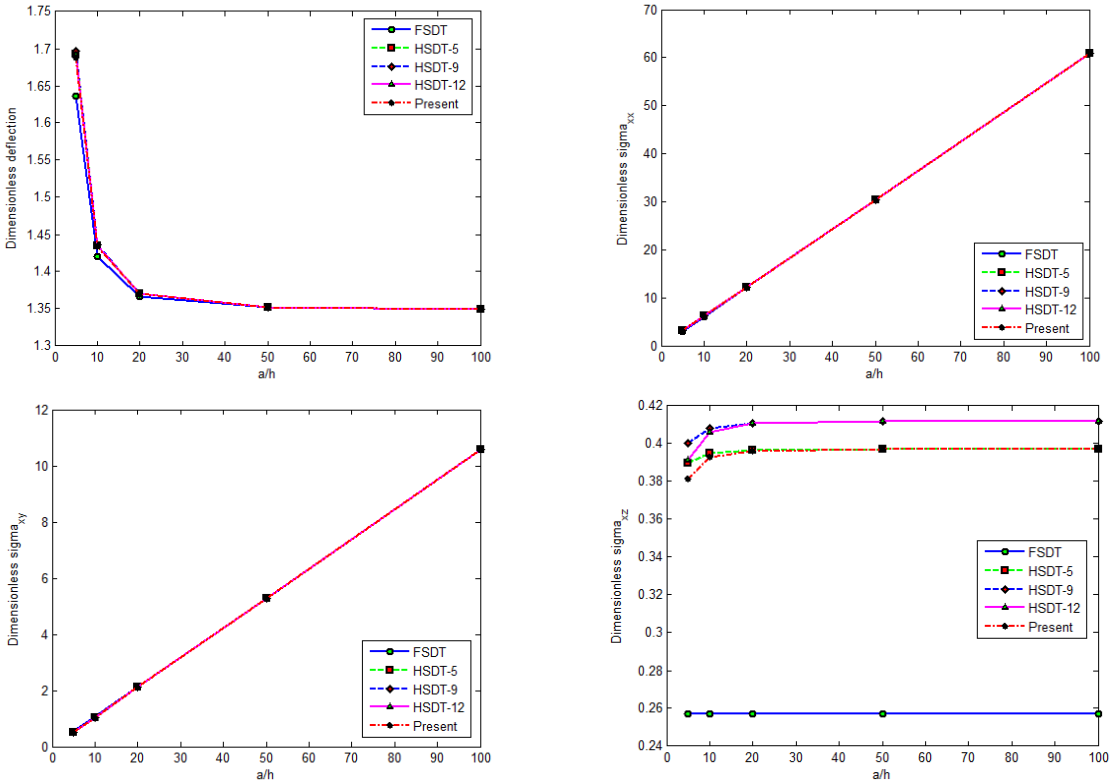

Fig. 4 Variation of dimensionless deflection $\bar{w}$, in-plane stresses $\bar{\sigma}_x, \bar{\sigma}_{xy}$, transverse stress $\bar{\sigma}_{xz}$ versus side-to-thickness ratio a/h of square plates under uniform loads (a=b, p=5)

Table 6 Dimensionless deflection and stresses of rectangular plates under uniform loads (a/h=10, p=5) with various value of aspect ratio b/a

b/a	Method	$\bar{w}$	$\bar{\sigma}_x(h/2)$	$\bar{\sigma}_y(h/3)$	$\bar{\sigma}_{xy}(-h/3)$	$\bar{\sigma}_{xz}(0)$	$\bar{\sigma}_{yz}(h/6)$
1	FSDT	1.4205	6.0843	1.6249	1.0579	0.2572	0.3577
	HSDT-5	1.4349	6.1411	1.6120	1.0466	0.3950	0.4883
	HSDT-9	1.4360	6.1573	1.6099	1.0447	0.4080	0.4861
	HSDT-12	1.4349	6.1649	1.6215	1.0494	0.4059	0.4871
	Present	**1.4338**	**6.1493**	**1.6240**	**1.0504**	**0.3930**	**0.4893**
2	FSDT	3.4736	12.9202	1.5719	1.5049	0.3570	0.3818
	HSDT-5	3.4960	13.0021	1.5649	1.4943	0.5490	0.5227
	HSDT-9	3.4976	13.0245	1.5637	1.4921	0.5678	0.5205
	HSDT-12	3.4960	13.0121	1.5843	1.4982	0.5657	0.5211
	Present	**3.4943**	**12.9902**	**1.5857**	**1.5002**	**0.5471**	**0.5236**
3	FSDT	4.1807	15.1016	1.3763	1.5378	0.3784	0.3724
	HSDT-5	4.2048	15.1891	1.3705	1.5282	0.5821	0.5102
	HSDT-9	4.2066	15.2129	1.3696	1.5260	0.6021	0.5082
	HSDT-12	4.2048	15.1963	1.3921	1.5323	0.6000	0.5085
	Present	**4.2030**	**15.1731**	**1.3933**	**1.5344**	**0.5801**	**0.5108**
4	FSDT	4.3768	15.6838	1.2994	1.5338	0.3825	0.3614
	HSDT-5	4.4012	15.7725	1.2939	1.5249	0.5885	0.4954
	HSDT-9	4.4031	15.7966	1.2930	1.5228	0.6087	0.4935
	HSDT-12	4.4013	15.7791	1.3159	1.5290	0.6066	0.4937
	Present	**4.3995**	**15.7557**	**1.3171**	**1.5311**	**0.5864**	**0.4959**
5	FSDT	4.4274	15.8291	1.2743	1.5257	0.3830	0.3504
	HSDT-5	4.4519	15.9180	1.2688	1.5174	0.5893	0.4804
	HSDT-9	4.4537	15.9421	1.2680	1.5154	0.6096	0.4786
	HSDT-12	4.4520	15.9246	1.2910	1.5215	0.6075	0.4788
	Present	**4.4501**	**15.9011**	**1.2921**	**1.5234**	**0.5873**	**0.4808**

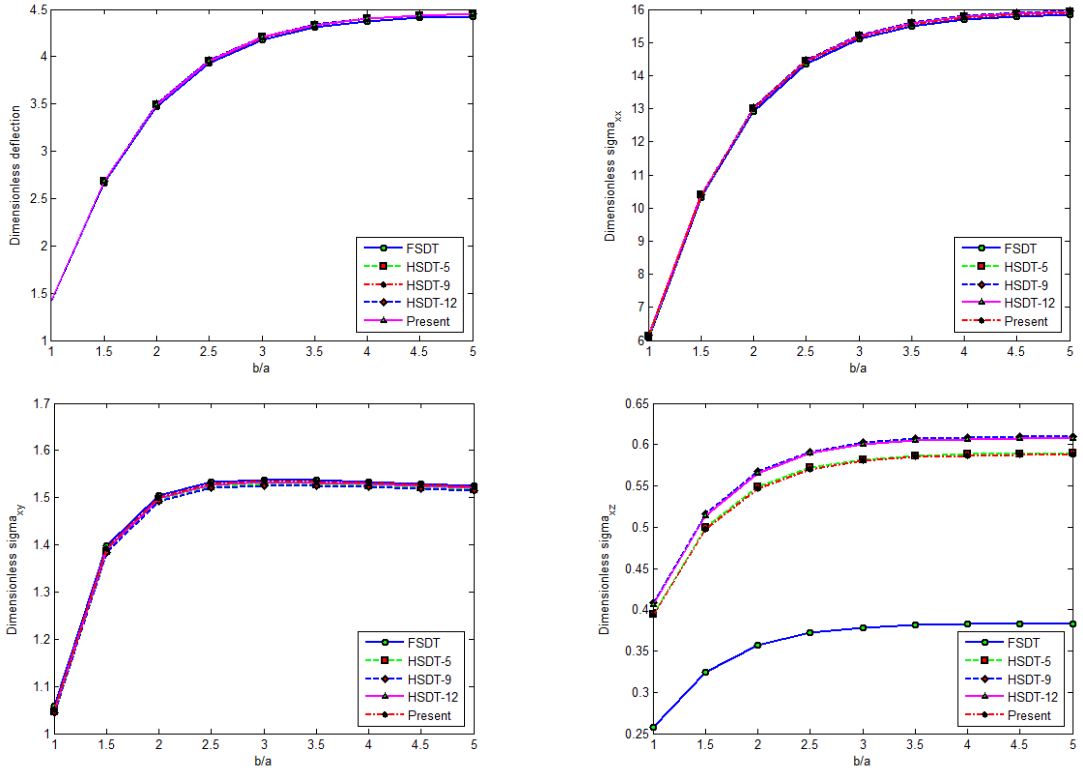

Fig. 5 Variation of dimensionless deflection $\bar{w}$, in-plane stresses $\bar{\sigma}_x, \bar{\sigma}_{xy}$, transverse stress $\bar{\sigma}_{xz}$ versus various aspect ratios b/a of rectangular plates under uniform loads (a=10h, p=5)

for transverse shear stress; there is a big difference between FSDT and HSDT results. Present eight-unknown HSDT results show good agreement with twelve-unknowns HSDT.

Example 3. A simply supported square FG plate under uniform load is considered. Table 5 shows dimensionless deflection and stresses with side-to-thickness ratio varies from 5 to 100 (p=5).

Fig. 4 presents the variation of dimensionless deflection $\bar{w}$, in-plane stresses $\bar{\sigma}_x, \bar{\sigma}_{xy}$, transverse stress $\bar{\sigma}_{xz}$ with respect to a/h ratio. It can be seen that the proposed new HSDT and full HSDT give almost identical results of deflections as well as tresses for all values of side-to-thickness ratio. The difference of deflection and transverse stress between FSDT and HSDT increases when the side-to-thickness ratio decreases.

The presented results on Table 5 and the graph in Figure 4 also show that for thick plates (a/h=5), the proposed HSDT gives more accurate results in comparison with FSDT and other HSDT. The consideration of a non-zero normal strain ε_z produces greater differences in the transverse shear stresses between present HSDT and FSDT, HSDT-5, HSDT-9. The effect of the zero transverse shear stresses at the top and bottom surfaces is evident by close results between proposed HSDT and HSDT-5 for σ_{xz}, σ_{yz}.

Example 4. A simply supported square FG plate under uniform load is considered (a/h=10, p=5). Dimensionless deflection and stresses with various aspect ratios are given in Table 6. The variation of dimensionless deflection and stresses with aspect ratio is plotted in Fig. 5. As can be seen from the results, the computations based on the present eight-unknown HSDT are again in good agreement with those predicted by other HSDT. The deflection and stresses increase as the aspect ratio increases. There is a bigger difference of transverse stresses between the present HSDT results and those predicted by full HSDT-12.

7. Conclusions

The new eight-unknown HSDT is proposed based on full twelve-unknown HSDT and satisfies vanishing transverse stresses at the top and bottom surface of FG plates. Static behavior of simply supported FG plates is studied, the deflection and stresses under uniformly distributed loading is analyzed. The accuracy of numerical solutions has been established with respect to known results in available literatures. The present HSDT gives more accurate results for thick FG plates than other HSDT by taking to account the normal stretching stresses and zeros transverse shear stresses on the top and bottom surfaces of FG plates. Additionally, the presented formulation for FG plates involves smaller computation compared to full twelve-unknown higher-order shear deformation theory. The numerical results for uniform loading should serve as a reference for any other analytical/computational model of FG plates.

Acknowledgements

This research is funded by Vietnam National Foundation for Science and Technology Development (NAFOSTED) under grant number: 107.02-2015.14, and Ministry of Education and Training Foundation for Science and Technology Project.

References

Alieldin, S.S., Alshorbagy, A.E. and Shaat, M. (2011), "A first-order shear deformation finite element model for elastostatic analysis of laminated composite plates and the equivalent functionally graded plates", *Ain Shams Eng. J.l*, **2**(1), 53-62.

Apuzzo, A., Barretta, R. and Luciano, R. (2015), "Some analytical solutions of functionally graded Kirchhoff plates", *Compos. Part B: Eng.*, **68**, 266-269.

Arani, A.G., Kolahchi, R. and Esmailpour, M. (2016), "Nonlinear vibration analysis of piezoelectric plates reinforced with carbon nanotubes using DQM", *Smart Struct. Syst.*, **18**(4), 787-800.

Barretta, R. and Luciano, R. (2014), "Exact solutions of isotropic viscoelastic functionally graded Kirchhoff plates", *Compos. Struct.*, **118**, 448-454.

Baseri, V., Jafari, G.S. and Kolahchi, R. (2016), "Analytical solution for buckling of embedded laminated plates based on higher order shear deformation plate theory", *Steel Compos. Struct.*, **21**(4), 883-919.

Birman, V. and Byrd, L.W. (2007), "Modeling and analysis of functionally graded materials and structures", *Appl. Mech. Rev.*, **60**(5), 195-216.

Carrera, E., Brischetto, S. and Robaldo, A. (2008), "Variable kinematic model for the analysis of functionally graded material plates", *AIAA J.*, **46**(1), 194-203.

Carrera, E., Brischetto, S., Cinefra, M. and Soave, M. (2011), "Effects of thickness stretching in functionally graded plates and shells", *Compos. Part B: Eng.*, **42**(2), 123-133.

Chi, S.H. and Chung, Y.L. (2006), "Mechanical behavior of functionally graded material plates under transverse load - Part I: Analysis", *Int. J. Solid. Struct.*, **43**(13), 3657-3674.

Della Croce, L. and Venini, P. (2004), "Finite elements for functionally graded Reissner-Mindlin plates", *Comput. Meth. Appl. Mech. Eng.*, **193**(9), 705-725.

Hosseini-Hashemi, S., Fadaee, M. and Atashipour, S.R. (2011), "A new exact analytical approach for free vibration of Reissner-Mindlin functionally graded rectangular plates", *Int. J. Mech. Sci.*, **53**(1), 11-22.

Hosseini-Hashemi, S., Taher, H.R.D., Akhavan, H. and Omidi, M. (2010), "Free vibration of functionally graded rectangular plates using first-order shear deformation plate theory", *Appl. Math. Model.*, **34**(5), 1276-1291.

Jędrysiak, J. and Michalak, B. (2011), "On the modeling of stability problems for thin plates with functionally graded structure", *Thin Wall. Struct.*, **49**(5), 627-635.

Jha, D.K., Kant, T. and Singh, R.K. (2012), "Higher order shear and normal deformation theory for natural frequency of functionally graded rectangular plates", *Nucl. Eng. Des.*, **250**, 8-13.

Jha, D.K., Kant, T. and Singh, R.K. (2013), "A critical review of recent research on functionally graded plates", *Compos. Struct.*, **96**, 833-849.

Kolahchi, R., Bidgoli, A.M.M. and Heydari, M.M. (2015a), "Size-dependent bending analysis of FGM nano-sinusoidal plates resting on orthotropic elastic medium", *Struct. Eng. Mech.*, **55**(5), 1001-1014.

Kolahchi, R., Bidgoli, M.R., Beygipoor, G. and Fakhar, M.H. (2015b), "A nonlocal nonlinear analysis for buckling in embedded FG-SWCNT-reinforced microplates subjected to magnetic field", *J. Mech. Sci. Technol.*, **29**(9), 3669-3677.

Kolahchi, R., Hosseini, H. and Esmailpour, M. (2016b),

"Differential cubature and quadrature-Bolotin methods for dynamic stability of embedded piezoelectric nanoplates based on visco-nonlocal-piezoelasticity theories", *Compos. Struct.*, **157**, 174-186.

Kolahchi, R., Safari, M. and Esmailpour, M. (2016a), "Dynamic stability analysis of temperature-dependent functionally graded CNT-reinforced visco-plates resting on orthotropic elastomeric medium", *Compos. Struct.*, **150**, 255-265.

Lee, Y.Y., Zhao, X. and Reddy, J.N. (2010), "Postbuckling analysis of functionally graded plates subject to compressive and thermal loads", *Comput. Meth. Appl. Mech. Eng.*, **199**(25), 1645-1653.

Lü, C.F., Lim, C.W. and Chen, W. (2009), "Size-dependent elastic behavior of FGM ultra-thin films based on generalized refined theory", *Int. J. Solid. Struct.*, **46**(5), 1176-1185.

Lu, P., He, L., Lee, H. and Lu, C. (2006), "Thin plate theory including surface effects", *Int. J. Solid. Struct.*, **43**(16), 4631-4647.

Neves, A.M.A., Ferreira, A.J.M., Carrera, E., Cinefra, M., Roque, C.M.C., Jorge, R.M.N. and Soares, C.M.M. (2013), "Static, free vibration and buckling analysis of isotropic and sandwich functionally graded plates using a quasi-3D higher-order shear deformation theory and a meshless technique", *Compos. Part B*, **44**(1), 657-674.

Neves, A.M.A., Ferreira, A.J.M., Carrera, E., Roque, C.M.C, Cinefra, M., Jorge, R.M.N. and Soares, C.M.M. (2012), "A quasi-3d sinusoidal shear deformation theory for the static and free vibration analysis of functionally graded plates", *Compos. Part B: Eng.*, **43**, 711-725.

Nguyen, T.K., Sab, K. and Bonnet, G. (2008), "First-order shear deformation plate models for functionally graded materials", *Compos. Struct.*, **83**(1), 25-36.

Reddy, J.N. (2000), "Analysis of functionally graded plates", *Int. J. Numer. Meth. Eng.*, **47**(1-3), 663-684.

Shaat, M., Mahmoud, F.F., Alieldin, S.S. and Alshorbagy, A.E. (2013), "Finite element analysis of functionally graded nano-scale films", *Finite Elem. Anal. Des.*, **74**, 41-52.

Shaat, M., Mahmoud, F.F., Alshorbagy, A.E., Alieldin, S.S. and Meletis, E.I. (2012), "Size-dependent analysis of functionally graded ultra-thin films", *Struct. Eng. Mech.*, **44**(4), 431-448.

Singha, M.K., Prakash, T. and Ganapathi, M. (2011), "Finite element analysis of functionally graded plates under transverse load", *Finite Elem. Anal. Des.*, **47**(4), 453-460.

Swaminathan, K. and Naveenkumar, D.T. (2014), "Higher order refined computational models for the stability analysis of FGM plates - Analytical solutions", *Euro. J. Mech. A/Solid.*, **47**, 349 - 361.

Swaminathan, K., Naveenkumar, D.T., Zenkour, A.M. and Carrera, E. (2015), "Stress, vibration and buckling analyses of FGM plates-A state-of-the-art review", *Compos. Struct.*, **120**, 10-31.

Taj, M.G., Chakrabarti, A. and Sheikh, A.H. (2013), "Analysis of functionally graded plates using higher order shear deformation theory", *Appl. Math. Model.*, **37**(18), 8484-8494.

Talha, M. and Singh, B.N. (2010), "Static response and free vibration analysis of FGM plates using higher order shear deformation theory", *Appl. Math. Model.*, **34**(12), 3991-4011.

Thai, H.T. and Choi, D.H. (2013), "A simple first-order shear deformation theory for the bending and free vibration analysis of functionally graded plates", *Compos. Struct.*, **101**, 332-340.

Tounsi, A., Houari, M.S.A. and Benyoucef, S. (2013), "A refined trigonometric shear deformation theory for thermoelastic bending of functionally graded sandwich plate", *Aerosp. Sci. Technol.*, **24**(1), 209-220.

Touratier, M. (1991), "An efficient standard plate theory", *Int. J. Eng. Sci.*, **29**(8), 901-916.

Yahia, S.A., Atmane, H.A., Houari, M.S.A. and Tounsi, A. (2015), "Wave propagation in functionally graded plates with porosities using various higher-order shear deformation plate theories". *Struct. Eng. Mech.*, **53**(6), 1143-1165.

Yang, J. and Shen, H.S. (2001), "Dynamic response of initially stressed functionally graded rectangular thin plates", *Compos. Struct.*, **54**(4), 497-508.

Zenkour, A.M. (2005a), "A comprehensive analysis of functionally graded sandwich plates: Part 1- Deflection and stresses", *Int. J. Solid. Struct.*, **42**(18), 5224-5242.

Zenkour, A.M. (2005b), "A comprehensive analysis of functionally graded sandwich plates: Part 2- Buckling and free vibration", *Int. J. Solid. Struct.*, **42**(18), 5243-5258.

Zenkour, A.M. (2006), "Generalized shear deformation theory for bending analysis of functionally graded plates", *Appl. Math. Model.*, **30**(1), 67-84.

Zenkour, A.M. (2009), "The refined sinusoidal theory for FGM plates on elastic foundations", *Int. J. Mech. Sci.*, **5**(11), 869-880.

CC

Appendix A. Definition of coefficient in Eq. (16)

$$s_{11}=A_{11}\alpha^2+A_{44}\beta^2;\quad s_{12}=s_{21}=(A_{12}+A_{44})\alpha\beta;$$

$$s_{13}=s_{31}=-\frac{D_{11}c_2}{3}\alpha^3-\left(\frac{D_{12}c_2}{3}+\frac{2D_{44}c_2}{3}\right)\alpha\beta^2;$$

$$s_{14}=s_{41}=\left(B_{11}-\frac{D_{11}c_2}{3}\right)\alpha^2+\left(B_{44}-\frac{D_{44}c_2}{3}\right)\beta^2;$$

$$s_{15}=s_{51}=\left(B_{12}+B_{44}-\frac{D_{12}c_2}{3}-\frac{D_{44}c_2}{3}\right)\alpha\beta;$$

$$s_{16}=s_{61}=-\frac{C_{11}}{2}\alpha^3-A_{13}\alpha-\left(\frac{C_{12}}{2}+C_{44}\right)\alpha\beta^2;$$

$$s_{17}=s_{71}=-\frac{D_{11}}{3}\alpha^3-2B_{13}\alpha-\left(\frac{D_{12}}{3}+\frac{2D_{44}}{3}\right)\alpha\beta^2;$$

$$s_{18}=s_{81}=-\frac{C_{11}c_1}{2}\alpha^3-3C_{13}\alpha-\left(\frac{C_{12}c_1}{2}+C_{44}c_1\right)\alpha\beta^2;\quad s_{22}=A_{44}\alpha^2+A_{22}\beta^2;$$

$$s_{23}=s_{32}=-\left(\frac{D_{21}c_2}{3}+\frac{2D_{44}c_2}{3}\right)\alpha^2\beta-\frac{D_{22}c_2}{3}\beta^3;$$

$$s_{24}=s_{42}=\left(B_{21}+B_{44}-\frac{D_{21}c_2}{3}-\frac{D_{44}c_2}{3}\right)\alpha\beta;$$

$$s_{25}=s_{52}=\left(B_{44}-\frac{D_{44}c_2}{3}\right)\alpha^2+\left(B_{22}-\frac{D_{22}c_2}{3}\right)\beta^2;$$

$$s_{26}=s_{62}=-\left(\frac{C_{21}}{2}+C_{44}\right)\alpha^2\beta-A_{23}\beta-\frac{C_{22}}{2}\beta^3;$$

$$s_{27}=s_{72}=-\left(\frac{D_{21}}{3}+\frac{2D_{44}}{3}\right)\alpha^2\beta-2B_{23}\beta-\frac{D_{22}}{3}\beta^3;$$

$$s_{28}=s_{82}=-\left(\frac{C_{21}c_1}{2}+C_{44}c_1\right)\alpha^2\beta-3C_{23}\beta-\frac{C_{22}c_1}{2}\beta^3;$$

$$s_{33}=\frac{G_{11}c_2^2}{9}\alpha^4+\left(A_{55}+E_{55}c_2^2-2C_{55}c_2\right)\alpha^2+\frac{(G_{12}+G_{21}+4G_{44})c_2^2}{9}$$

$$\alpha^2\beta^2+\left(A_{66}+E_{66}c_2^2-2C_{66}c_2\right)\beta^2+\frac{G_{22}c_2^2}{9}\beta^4;$$

$$s_{34}=s_{43}=\left(\frac{G_{11}c_2^2}{9}-\frac{E_{11}c_2}{3}\right)\alpha^3+\left(A_{55}-2C_{55}c_2+E_{55}c_2^2\right)\alpha$$

$$-\left(\frac{E_{21}c_2}{3}+\frac{2E_{44}c_2}{3}-\frac{G_{21}c_2^2}{9}-\frac{2G_{44}c_2^2}{9}\right)\alpha\beta^2;$$

$$s_{35}=s_{53}=-\left(\frac{E_{12}c_2}{3}+\frac{2E_{44}c_2}{3}-\frac{G_{12}c_2^2}{9}-\frac{2G_{44}c_2^2}{9}\right)\alpha^2\beta$$

$$+\left(A_{66}-2C_{66}c_2+E_{66}c_2^2\right)\beta+\left(\frac{G_{22}c_2^2}{9}-\frac{E_{22}c_2}{3}\right)\beta^3;$$

$$s_{36}=s_{63}=\frac{F_{11}c_2}{6}\alpha^4+\frac{D_{13}c_2}{3}\alpha^2+$$

$$\left(\frac{F_{12}c_2}{6}+\frac{F_{21}c_2}{6}+\frac{2F_{44}c_2}{3}\right)\alpha^2\beta^2+\frac{D_{23}c_2}{3}\beta^2+\frac{F_{22}c_2}{6}\beta^4;$$

$$s_{37}=s_{73}=\frac{G_{11}c_2}{9}\alpha^4+\frac{2E_{13}c_2}{3}\alpha^2+$$

$$\left(\frac{G_{12}c_2}{9}+\frac{G_{21}c_2}{9}+\frac{4G_{44}c_2}{9}\right)\alpha^2\beta^2+\frac{2E_{23}c_2}{3}\beta^2+\frac{G_{22}c_2}{9}\beta^4;$$

$$s_{38}=s_{83}=\frac{F_{11}c_1c_2}{6}\alpha^4+\left(D_{55}-B_{55}c_1+F_{13}c_2-\right.$$

$$\left.F_{55}c_2+D_{55}c_1c_2\right)\alpha^2+\left(\frac{F_{12}c_1c_2}{6}+\frac{F_{21}c_1c_2}{6}+\frac{2F_{44}c_1c_2}{3}\right)\alpha^2\beta^2$$

$$+\left(D_{66}-B_{66}c_1+F_{23}c_2-F_{66}c_2+D_{66}c_1c_2\right)\beta^2+\frac{F_{22}c_1c_2}{6}\beta^4;$$

$$s_{44}=\left(\frac{G_{11}c_2^2}{9}-\frac{2E_{11}c_2}{3}+C_{11}\right)\alpha^2+$$

$$+\left(\frac{G_{44}c_2^2}{9}-\frac{2E_{44}c_2}{3}+C_{44}\right)\beta^2+E_{55}c_2^2-2C_{55}c_2+A_{55};$$

$$s_{45}=s_{54}=\left(C_{12}+C_{44}+\frac{G_{12}c_2^2}{9}+\frac{G_{44}c_2^2}{9}-\frac{2E_{12}c_2}{3}-\frac{2E_{44}c_2}{3}\right)\alpha\beta;$$

$$s_{46}=s_{64}=-\left(\frac{D_{11}}{2}-\frac{F_{11}c_2}{6}\right)\alpha^3+\left(\frac{D_{13}c_2}{3}-B_{13}\right)\alpha$$

$$-\left(\frac{D_{12}}{2}+D_{44}-\frac{F_{12}c_2}{6}-\frac{F_{44}c_2}{3}\right)\alpha\beta^2;$$

$$s_{47}=s_{74}=-\left(\frac{E_{11}}{3}-\frac{G_{11}c_2}{9}\right)\alpha^3+\left(\frac{2E_{13}c_2}{3}-2C_{13}\right)\alpha$$

$$-\left(\frac{E_{12}}{3}+\frac{2E_{44}}{3}-\frac{G_{12}c_2}{9}-\frac{2G_{44}c_2}{9}\right)\alpha\beta^2;$$

$$s_{48}=s_{84}=-\left(\frac{D_{11}c_1}{2}-\frac{F_{11}c_1c_2}{6}\right)\alpha^3+\left(D_{55}-3D_{13}-B_{55}c_1+F_{13}c_2-\right.$$

$$\left.F_{55}c_2+D_{55}c_1c_2\right)\alpha-\left(\frac{D_{12}c_1}{2}+D_{44}c_1-\frac{F_{12}c_1c_2}{6}-\frac{F_{44}c_1c_2}{3}\right)\alpha\beta^2;$$

$$s_{55}=\left(\frac{G_{44}c_2^2}{9}-\frac{2E_{44}c_2}{3}+C_{44}\right)\alpha^2+$$

$$\left(\frac{G_{22}c_2^2}{9}-\frac{2E_{22}c_2}{3}+C_{22}\right)\beta^2+E_{66}c_2^2-2C_{66}c_2+A_{66};$$

$$s_{56}=s_{65}=-\left(\frac{D_{21}}{2}+D_{44}-\frac{F_{21}c_2}{6}-\frac{F_{44}c_2}{3}\right)\alpha^2\beta$$

$$+\left(\frac{D_{23}c_2}{3}-B_{32}\right)\beta-\left(\frac{D_{22}}{2}-\frac{F_{22}c_2}{6}\right)\beta^3;$$

$$s_{57}=s_{75}=-\left(\frac{E_{21}}{3}+\frac{2E_{44}}{3}-\frac{G_{21}c_2}{9}-\frac{2G_{44}c_2}{9}\right)\alpha^2\beta$$

$$+\left(\frac{2E_{23}c_2}{3}-2C_{23}\right)\beta-\left(\frac{E_{22}}{3}-\frac{G_{22}c_2}{9}\right)\beta^3;$$

$$s_{58}=s_{85}=-\left(\frac{D_{21}c_1}{2}+D_{44}c_1-\frac{F_{21}c_1c_2}{6}-\frac{F_{44}c_1c_2}{3}\right)\alpha^2\beta+\left(D_{66}-3D_{23}-\right.$$

$$\left.B_{66}c_1+F_{23}c_2-F_{66}c_2+D_{66}c_1c_2\right)\beta-\left(\frac{D_{22}c_1}{2}-\frac{F_{22}c_1c_2}{6}\right)\beta^3;$$

$$s_{66}=\frac{E_{11}}{4}\alpha^4+\left(\frac{C_{13}}{2}+\frac{C_{31}}{2}\right)\alpha^2+\left(\frac{E_{12}}{4}+\frac{E_{21}}{4}+E_{44}\right)\alpha^2\beta^2$$

$$+\left(\frac{C_{23}}{2}+\frac{C_{32}}{2}\right)\beta^2+\frac{E_{22}}{4}\beta^4+A_{33};$$

$$s_{67}=s_{76}=\frac{F_{11}}{6}\alpha^4+\left(D_{13}+\frac{D_{31}}{3}\right)\alpha^2+\left(\frac{F_{12}}{6}+\frac{F_{21}}{6}+\frac{2F_{44}}{3}\right)\alpha^2\beta^2$$

$$+\left(D_{23}+\frac{D_{32}}{3}\right)\beta^2+\frac{F_{22}}{6}\beta^4+2B_{33};$$

$$s_{68}=s_{86}=\frac{E_{11}c_1}{4}\alpha^4+\left(\frac{3E_{13}}{2}+\frac{C_{31}c_1}{2}\right)\alpha^2+\left(\frac{E_{12}c_1}{4}+\frac{E_{21}c_1}{4}+E_{44}c_1\right)\alpha^2\beta^2$$

$$+\left(\frac{3E_{23}}{2}+\frac{C_{32}c_1}{2}\right)\beta^2+\frac{E_{22}c_1}{4}\beta^4+3C_{33};$$

$$s_{77} = \frac{G_{11}}{9}\alpha^4 + \left(\frac{2E_{13}}{3} + \frac{2E_{31}}{3}\right)\alpha^2 + \left(\frac{G_{12}}{9} + \frac{G_{21}}{9} + \frac{4G_{44}}{9}\right)\alpha^2\beta^2$$

$$+ \left(\frac{2E_{23}}{3} + \frac{2E_{32}}{3}\right)\beta^2 + \frac{G_{22}}{9}\beta^4 + 4C_{33};$$

$$s_{78} = s_{87} = \frac{F_{11}c_1}{6}\alpha^4 + \left(F_{31} + D_{31}c_1\right)\alpha^2 + \left(\frac{F_{12}c_1}{6} + \frac{F_{21}c_1}{6} + \frac{2F_{44}c_1}{3}\right)\alpha^2\beta^2$$

$$+ \left(F_{32} + D_{32}c_1\right)\beta^2 + \frac{F_{22}c_1}{6}\beta^4 + 6D_{33};$$

$$s_{88} = \frac{E_{11}c_1^2}{4}\alpha^4 + \left(G_{55} + C_{55}c_1^2 + \frac{3E_{13}c_1}{2} + \frac{3E_{31}c_1}{2} - 2E_{55}c_1\right)\alpha^2 \cdot$$

$$+ \left(\frac{E_{12}c_1^2}{4} + \frac{E_{21}c_1^2}{4} + E_{44}c_1^2\right)\alpha^2\beta^2 +$$

$$\left(G_{66} + C_{66}c_1^2 + \frac{3E_{23}c_1}{2} + \frac{3E_{32}c_1}{2} - 2E_{66}c_1\right)\beta^2 + \frac{E_{22}c_1^2}{4}\beta^4 + 9E_{33}.$$